RESEARCH ARTICLE | DECEMBER 29 2021

Functionalized carbon nanotubes for thermionic emission and cooling applications

Special Collection: Functional Coatings

Feng Jin ✉; Ansibert Miruko; Daniel Litt; Karolena Zhou

Journal of Vacuum Science & Technology A 40, 013415 (2022)
https://doi.org/10.1116/6.0001467
CHORUS

Related Content

High thermionic emission from barium strontium oxide functionalized carbon nanotubes thin film surface

Appl. Phys. Lett. (May 2017)

Thermionic emission from carbon nanotubes with a thin layer of low work function barium strontium oxide surface coating

Appl. Phys. Lett. (April 2006)

Barium strontium oxide functionalized carbon nanotubes thin film thermionic emitter with superior thermionic emission capability

Journal of Vacuum Science & Technology B (May 2017)

JVST A
Journal of Vacuum Science & Technology A

ARTICLE

avs.scitation.org/journal/jva

Functionalized carbon nanotubes for thermionic emission and cooling applications

Cite as: J. Vac. Sci. Technol. A **40**, 013415 (2022); doi: 10.1116/6.0001467
Submitted: 15 September 2021 · Accepted: 10 December 2021 ·
Published Online: 29 December 2021

Feng Jin,[1,a)] Ansibert Miruko,[1] Daniel Litt,[1] and Karolena Zhou[2]

AFFILIATIONS

[1]Department of Physics and Astronomy, Ball State University, Muncie, Indiana 47306
[2]Carmel High School, Carmel, Indiana 46032

Note: This paper is a part of the Special Topic Collection on Functional Coatings.
[a)]**Author to whom correspondence should be addressed:** fjin@bsu.edu

ABSTRACT

Barium strontium oxide-coated carbon nanotubes (CNTs) were implemented as a work function lowering and field enhancing functional coating on a coiled tungsten filament to create a new thermionic cathode. This cathode resembles conventional oxide cathodes in structure. It has the same coiled tungsten filament as a conventional oxide cathode but uses barium strontium oxide-coated CNTs instead of the traditional barium strontium calcium oxide powder mixture as an emissive coating. The cathode produces a strong thermionic emission. At 1395 K and 2.5 V/μm, the thermionic emission current of 0.87 A or current density of 2.9 A/cm^2 was obtained from this oxide-coated CNT cathode. This level of emission is about three times as large as a conventional oxide cathode operating at similar temperature and field strength. Strong thermionic emissions from the cathode also lead to a large thermionic cooling effect. Temperature reduction as large as 90° was observed from the cathode surface when it was emitting electrons. Strong thermionic emission and a large cooling effect obtained are the result of the combination of the low work function of barium strontium oxide (1.6 eV) and the large field effect induced by the CNTs. Plasma enhanced chemical vapor deposition was used to grow CNTs, and magnetron sputtering deposition was used to deposit the barium strontium oxide functional coating; details of the cathode fabrication are presented to illustrate both the versatility of the processing techniques and the adaptability of barium strontium oxide-coated CNTs as a functional coating. Measurements on thermionic emission and thermionic cooling of the cathode are also presented.

I. INTRODUCTION

Carbon nanotubes (CNTs) are an interesting material that has many unique electrical, mechanical, thermal, and chemical properties. CNTs are also excellent electron emitters due to their unique geometry and high aspect ratio, which induces a high field enhancement factor around their tips. Because of this large field enhancement effect, most studies of electron emission from CNTs focus on field emission.[1–5] However, they have not been explored as extensively as thermionic emitters, even though a large field effect is also highly beneficial in thermionic emission.[6–10]

Thermionic emission is described by the Richardson equation as follows:[11,12]

$$J_s = A_{\text{eff}} T^2 e^{-11605\varphi/T} e^{4.4\sqrt{E}/T}, \tag{1}$$

where J_s is the saturation current density, T is the temperature of the emission surface in Kelvin, φ is the work function of the emission surface in electron volts, E is the electric field on the emission surface in V/cm, and A_{eff} is the effective Richardson's constant, with the theoretical value of 120 A/K^2 cm^2 for metals. The first part of the equation is also referred to as the zero-field emission current density J_0, which is the amount of emission produced without the presence of an electric field,

$$J_0 = A_{\text{eff}} T^2 e^{-11605\varphi/T}. \tag{2}$$

The last exponential term, $e^{4.4\sqrt{E}/T}$, in Eq. (1) is the field effect in thermionic emission known as the Schottky effect. Apparently, a large field effect can have a direct and significant impact on thermionic emissions. CNTs have a large field effect that can help

boost thermionic emission, but the problem with CNTs being thermionic emitters is that they have a large work function.[7,10] As can be seen from the Richardson equation, a large work function hinders thermionic emission and makes CNTs weak thermionic emitters.[6–10]

Fortunately, it is possible to modify the CNTs surface with a functional coating. CNT surfaces have been altered and their properties enhanced with various functional coatings by many researchers for different applications.[13–16] Previously, we have also shown that the work function of the CNT surface can be significantly lowered by depositing a low work function barium strontium oxide thin film on top of it. The reduction of work function coupled with the large field enhancement effect induced by the CNTs results in strong thermionic emissions from these functionalized CNTs.[17,18]

However, in our earlier work, barium strontium oxide-coated CNTs were grown and deposited on a flat surface. While their thermionic emission properties have been characterized and studied in detail; they have not been implemented in practical thermionic devices.[17,18] Real thermionic devices often have more complex structures and the ability of an emissive coating to be incorporated into such structures is important. In this study, we show the implementation of barium strontium oxide-coated CNTs on a rather complex filament structure and present a practical thermionic cathode based on this material. Thermionic cathodes are widely used in many applications such as x-ray machines in the medical field, microwave (and millimeter wave) traveling wave tubes (TWTs) for space communications, linear accelerators in high-energy physics, and florescent lamps and other gas electronics devices.[12,19–21] They are an integral part of the devices that provide strong and stable electron supplies. Thermionic cathodes come in various forms, and there are three major types of thermionic cathodes: metal cathodes, oxide cathodes, and dispense cathodes.[19] Metal cathodes are made of refractory metals such as tungsten (W) that are designed to operate at very high temperatures. Oxide cathodes consist of a heating element and an oxide coating (typically, in the form of a BaO, SrO, and CaO powder mixture) on it as electron emitters. Dispense cathodes are made of a disk formed by a matrix of tungsten and oxide powders compressed together. The cathode presented in this study resembles oxide cathodes widely used in fluorescent lamps these days.[22–29] It has a coiled tungsten filament as the base cathode structure, the same as in the conventional oxide cathodes but uses barium strontium oxide-coated CNTs as an emissive coating instead of the BaO, SrO, and CaO powder mixture in conventional oxide cathodes. Details of the fabrication of the cathode and its thermionic emission characteristics are reported in Secs. II–III.

The ability for barium strontium oxide-coated CNTs to be incorporated into a complex structure implies that they can potentially be implemented as a work function lowering and field enhancing functional coating in other devices and applications as well. One of these possible applications is thermionic cooling. With the ever-increasing power densities of electronic devices these days, cooling of power electronics becomes a major issue.[30–32] Many cooling schemes are being explored to meet this challenge; thermionic cooling is one of them.[33–38] Thermionic cooling occurs when hot electrons are ejected from the surface carrying energy away. The key to achieve a large thermionic cooling effect is to have a strong thermionic emission from the surface. A large thermionic cooling effect on a flat tungsten surface with a barium strontium oxide-coated CNTs on it has been observed and reported previously.[37,38] Here in this paper, we report a thermionic cooling effect that occurred on a more complex coiled filament cathode surface. It serves as another example of the adaptability and versatility of barium strontium oxide-coated CNTs as a functional coating for potential thermionic cooling devices and applications.

II. EXPERIMENT

A. Fabrication of thermionic cathodes

Triple coiled tungsten filaments were used as the base cathode structures for the thermionic cathodes fabricated in this study. These filaments are made of thin tungsten wires, which are designed to hold emissive oxide powders and be heated up directly when an electric current is flown through. The tungsten filaments used in this study were supplied by GE Company, and they are the same filaments used in some of the commercial compact fluorescent lamp products. CNTs were grown directly on these tungsten filaments using plasma enhanced chemical vapor deposition (PECVD). The tungsten filaments were thoroughly cleaned in dilute acids and solvents before the growth of CNTs. A thin catalytic film of nickel, about 100 nm, was first sputter deposited on the surface of the tungsten filament using magnetron sputtering deposition, after which, the filament was transferred to a PECVD chamber to be annealed and etched in NH_3 plasma at 650 °C for about 15 min to form nickel islands on its surface. These catalytic nickel islands serve as seeds for the CNT growth. C_2H_2 and NH_3 gases, at 1:2 ratio, were then flown to the PECVD chamber to start the CNT growth. The growth temperature was maintained at 650 °C, while the plasma power supplied by an Advanced Energy MDX 500 power supply was set at 50 W throughout the growth process. The length of the CNTs was controlled by the growth time, which was set at 15 min in this study to yield CNTs about 10–20 μm in length. The growth of CNTs on the surface of the tungsten filament was confirmed with scanning electron microscopy (SEM) and transmission electron microscopy (TEM).

The tungsten filament was transferred back to the sputtering chamber after the CNT growth. Barium strontium oxide thin film was deposited onto the CNT surface using magnetron sputtering deposition. Two pure barium and pure strontium sputtering targets mounted on two independent sputtering guns were cosputtered in an Ar/O_2 (at 5:1 ratio) ambient. The base pressure of the sputtering system was approximately 5×10^{-7} Torr. The pressure of the sputtering chamber was at about 1 mTorr during the deposition. Two Dressler CESAR 136 RF power supplies were used to supply power to the barium and strontium targets at 75 W and 50 W, respectively, which resulted in a thin film with a chemical composition of approximately 70% BaO and 30% SrO in molecular weight. The thickness of the barium strontium oxide thin film was monitored with a quartz crystal thin-film thickness monitor, the deposition time was approximately 30 min, which produced an oxide coating about 50 nm thick. The tungsten filament was placed on a heated rotating stage during the deposition. The growth temperature was set at 700 °C and the substrate stage rotated at 20 rpm during the deposition. The formation of a barium strontium oxide thin film

on CNTs' surface was examined and confirmed with SEM, TEM, and energy dispersive x-ray spectroscopy (EDS).

B. Measurements of thermionic emission

Thermionic emissions of the cathodes at various temperatures and field strengths were measured in a custom ultrahigh vacuum system with the base vacuum less than 5×10^{-8} Torr. The emission data collected were used to extract the work functions of cathodes. Figure 1 shows the schematic of the ultrahigh vacuum system. In this measurement system, the cathode being measured was mounted on the opposite side of the anode in a simple diode arrangement. The position of the cathode was fixed, while the anode, which also serves as the heatsink, was attached to movable electric feedthrough that controls the spacing between the cathode and anode. In this study, the spacing between the cathode and anode was fixed at 0.1 cm for every measurement. An electric field across the cathode and anode was established by supplying a voltage across the cathode and anode using a Glassman PS/LQ05P2 high voltage power supply; the electric field strength can be calculated by dividing the electric potential across and the spacing between the cathode and anode, in doing so, we assume the space-charge effect is minimum in our experimental setting. The electron emission from the cathode was measured using a Keithley 2700 multimeter; An Agilent E3631A source-measurement unit was used to heat the cathode to an elevated temperature by flowing a current through it. A Pyro MicroTherm optical pyrometer, sold by the Pyrometer Instrument Co. of Trenton, New Jersey, was used to measure the temperature of the cathode through the viewing window from outside of the ultrahigh vacuum system. The Glassman high voltage power supply, the Keithley Multimeter, and the Agilent source-measurement unit were connected to a computer and the data collections were controlled by a LABVIEW program.

Thermionic emissions of the cathodes were characterized in terms of their thermionic emission current at various temperatures and electric field strengths. For each cathode tested, emissions at seven different thermionic emission temperature levels were measured. For each set of measurements at a particular temperature, an electric current was flown through the cathode using the Agilent source-measurement unit to raise the temperature of the cathode to a predetermined target level. The LABVIEW program controls and adjusts the electric current level based on the relative change of the resistance of the hot cathode until the targeted temperature was reached. The more exact cathode temperature was then determined using the Pyro optical pyrometer. Once the cathode temperature was set, the Glassman high voltage power supply was then used to raise the electric potential across the cathode and anode, and the electron emission currents at various electric potentials measured. Five current measurements were taken with the Keithley multimeter at each bias voltage, and the average current was recorded. Each set of measurements produced an emission current versus electric potential (I-V) curve at that particular cathode temperature. For each cathode tested, thermionic emission measurements were performed at seven different temperatures, so a set of seven I-V curves at seven different cathode temperatures was obtained for each cathode. Work functions of the cathodes were extracted from these I-V curves using the Richardson line method.[11,12]

C. Measurements of thermionic cooling effect

The cooling of the cathode surface due to thermionic emission was measured in the same ultrahigh vacuum system shown in Fig. 1. The temperature of the cathode was raised by flowing an electric current through it using the Agilent source-measurement unit. The temperature of the cathode when it was not emitting electrons was measured first. The electrical potential across the cathode and anode supplied by the Glassman high voltage power supply was then turned on (for this study, the applied voltage was at a fixed value of 2500 V), and the temperature of the cathode was measured again when it was emitting electrons. The first temperature measured is referred to as the temperature of the cathode when emission is off, and the second temperature measured is the temperature of the cathode when emission is on. The difference of these two temperatures is the cooling effect caused by thermionic emission from the cathode surface. The Pyro optical pyrometer was used to measure cathode temperature precisely. Inside the optical pyrometer, there is a fine reference filament. By overlapping the reference filament with the center of the cathode being measured through the build-in telescope and adjusting the temperature of the reference filament to match that of the cathode, the temperature of the cathode can be determined. Five temperature readings were taken and averaged for every temperature measurement. The measurements are fairly consistent with only a few degrees of variation between readings once eyes are trained and adjusted in the dark environment. More details of the measurement techniques and procedures are also available in Refs. 37 and 38. In this study, cooling of the cathodes at seven temperature levels was assessed.

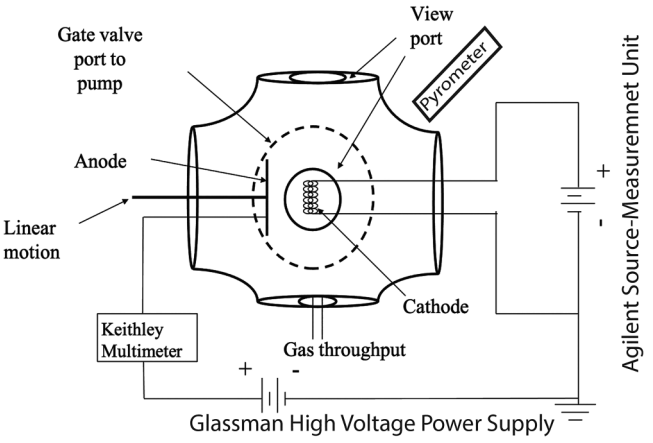

FIG. 1. Schematic of the experimental setup for thermionic emission and thermionic cooling measurement. The source-measurement unit is connected to the cathode and used to resistively heat it to high temperature by sending a current through the cathode. The Glassman high voltage power supply provides the bias voltage between the cathode and anode, and the Keithley multimeter measures the emission current from the cathode to anode. Cathode temperature is measured using the Pyro optical pyrometer pointed at the cathode from outside of the system.

III. RESULTS AND DISCUSSIONS

A. Triple coiled tungsten filament CNT cathodes

The structure of the coiled tungsten filaments used to fabricate the cathodes is shown in Fig. 2(a). As described in Sec. II, these tungsten filaments are used for the CNT growth and subsequent barium strontium oxide deposition. So, Fig. 2(a) also shows the overall structure of all the cathodes fabricated in this study. Such a coiled tungsten filament is widely used as the base structure for oxide cathodes, the fine tungsten coils are designed for holding emissive materials and allowing effective resistive heating of the cathode to thermionic emission temperatures.[22–24] The tungsten filaments used in this study were supplied by GE Company. Multiple cathodes were fabricated. Figure 2(b) is a SEM image of a segment of a cathode with barium strontium oxide-coated CNTs on it, the CNTs shown in the SEM micrograph are functionalized with barium strontium oxide coating. As can be seen from the image, the cathode surface is fully covered with the oxide-coated CNTs. Figure 2(c) shows an SEM image of a magnified segment of the cathode that provides a closer look at the CNTs grown on the cathode surface. The CNTs shown in this SEM micrograph are uncoated, as they were first grown on the tungsten filament surface using PECVD and before the subsequent functionalization with the barium strontium oxide coating. Figure 2(d) is another SEM image of a magnified segment of the cathode with barium strontium oxide-coated CNTs on its surface. These oxide-coated CNTs are about 200–300 nm in diameter and around 10–20 μm in length. The thickness of the barium strontium coating on the CNTs is around 50 nm.

The thickness of the barium strontium oxide coating was controlled by the deposition time and the thin-film thickness monitor. Figure 3(a) is a TEM image of an individual barium strontium oxide-coated CNT, the oxide coating on the CNT surface can be clearly seen in the image. Figure 3(b) shows the EDS of the cathode, all the chemical elements, Ba, Sr, C, O, and W, can be identified in the spectrum, which further confirms the formation of barium strontium oxide-coated CNTs on the cathode surface.

This cathode resembles a typical oxide cathode in the structure. They both use coiled tungsten filaments as the base structure,

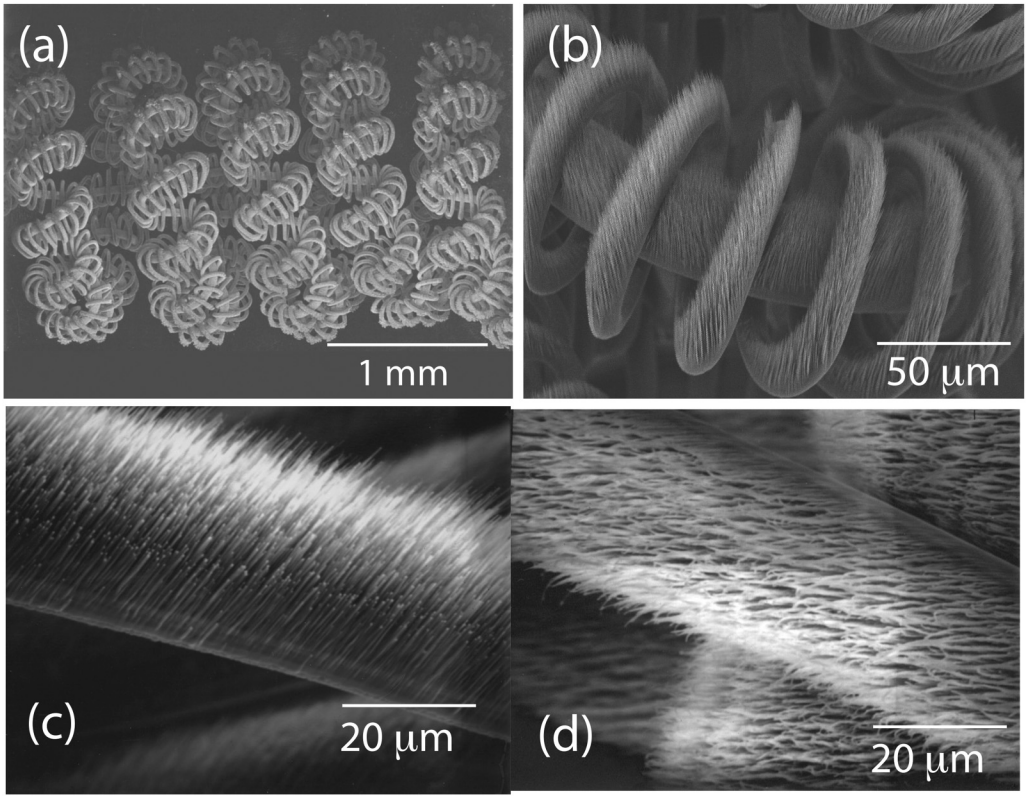

FIG. 2. (a) SEM image of a coiled tungsten filament used as the base structure for the cathode. (b) A segment of a barium strontium oxide-coated CNTs filament cathode. In the image, oxide-coated CNTs can be seen on the surface of the filament. CNTs were grown directly onto the surface and subsequently coated with barium strontium oxide using magnetron sputtering deposition. (c) An enlarged segment of the cathode with CNTs on the filament surface. The CNTs in the image are uncoated. (d) An enlarged segment of a barium strontium CNTs filament cathode that provides a close look at the oxide-coated CNTs on the cathode surface, the CNTs are about 10–20 μm in length.

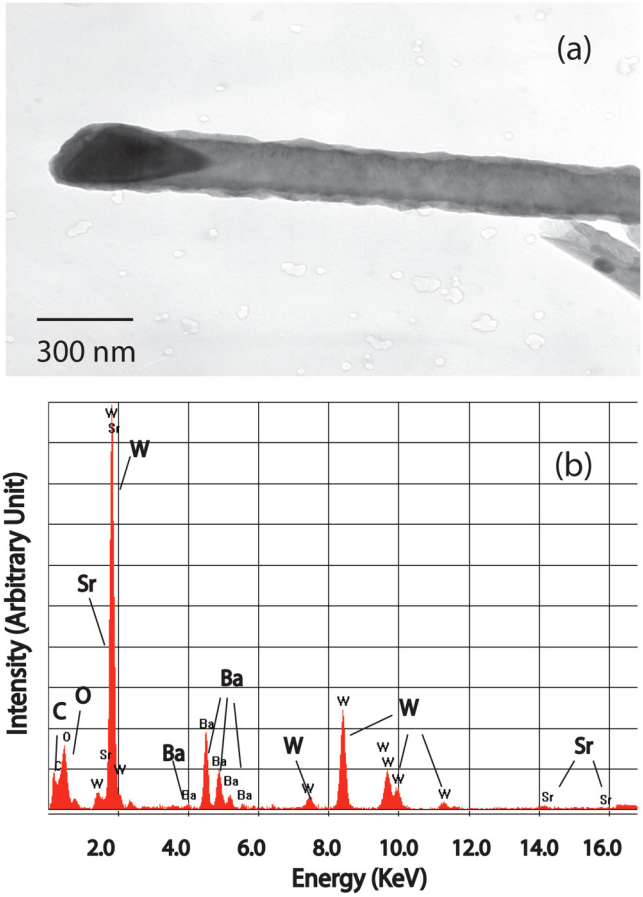

FIG. 3. (a) TEM micrograph of a barium strontium oxide-coated CNT; the barium strontium oxide thin film coating on the CNT can be seen from the image. The CNT shown is about 200 nm in diameter, and the barium strontium coating is about 50 nm thick. (b) An EDS spectrum showing the chemical composition of the cathode surface. Elements of tungsten, carbon, oxygen, barium, and strontium are identified.

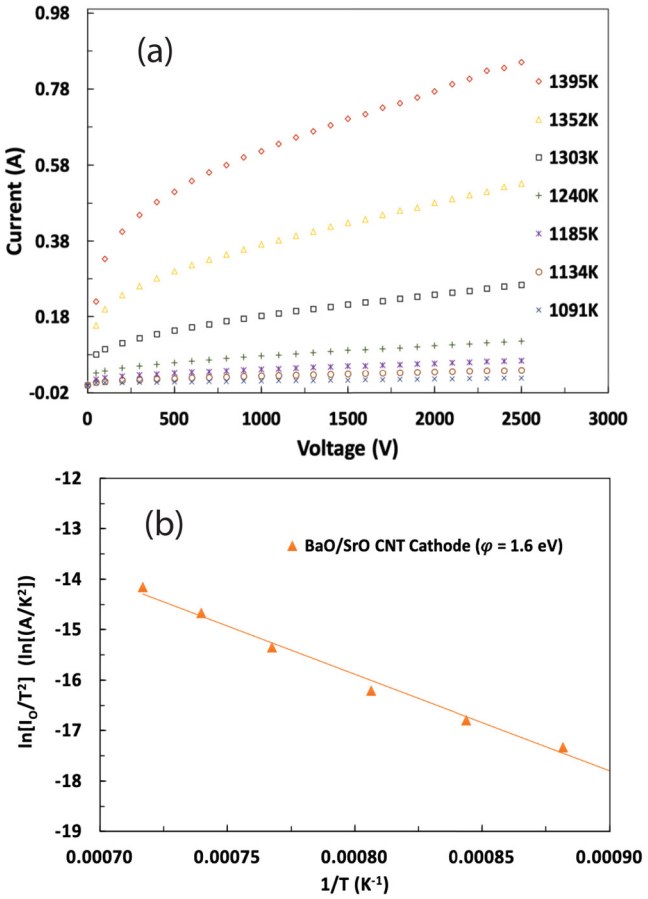

FIG. 4. (a) Thermionic emission current of the barium strontium oxide-coated CNT cathode as a function of electric potential bias at various temperatures. Each current data point represents the average of five measurements. (b) The corresponding Richardson plot of the thermionic emission. The y axis of the Richardson plot is the natural logarithm of the zero-field emission current divided by square of temperature.

meaning that this cathode can be heated up to thermionic emission temperatures similarly as a conventional cathode in typical operating conditions, which makes it easier for adoption as an alternative to a conventional oxide cathode. The difference between this cathode and a conventional oxide cathode is in the emissive materials coatings. A conventional oxide cathode uses oxide powder mixture as the emissive materials coating[22–24,29] versus in this cathode, it uses barium strontium oxide-coated CNTs as the emissive materials coating.

In addition to its potential application in thermionic cathodes, the ability to grow CNTs on a complex coiled filament structure and further functionalize them with a barium strontium oxide coating illustrates the versatility of the growth and fabrication techniques for producing this material, as well as the adaptability of barium strontium oxide as a functional coating in device applications. It is conceivable that barium strontium oxide may find applications in other devices as a work function lowering and field enhancing functional coating.

B. Thermionic emissions of the cathodes

Thermionic emissions from the cathode and the work function of the cathode surface are shown in Fig. 4. Each I-V curve in Fig. 4(a) corresponds to the thermionic emission current of the cathode at various potentials across the cathode and anode at a given cathode temperature. The voltages across the cathode and anode various from 0 to 2500 V. Given that the spacing between the cathode and anode is 0.1 cm, the electric field across the cathode and anode can be estimated as varied from 0 to 2.5 V/μm during the measurements. Again, in making this estimate, we neglect the space-charge effect. Typically, thermionic emission transitions from the space-charge limited (SCL) region at lower

fields to the temperature limited (TL) region as field strength increases. The space-charge effect tends to be more significant at the lower field strength but less so at the higher field strength in thermionic emission.[21,39] As shown in these I-V curves, thermionic emission from the cathode surface increases with field strength and temperature. The initial rise of emission current is steep, and it starts to enter the saturation region as field increases further to a certain level, which is expected from a thermionic cathode. The highest emission current obtained from the cathode is 0.87 A, at 1395 K and 2.5 V/μm, which is the highest temperature and field strength applied.

This is a very strong thermionic emission, particularly, in comparison with conventional oxide cathodes in similar operating conditions in fluorescent lamps.[22–28] Conventional oxide cathodes widely used in fluorescent lamps these days have a similar coiled tungsten filament cathode. The temperatures of conventional cathodes vary with the operating conditions, such as the lamp current that the cathode supplies, but they are typically around 1400 K,[22–26] and the electric field strengths in front of the cathode in discharge plasma are around 2.9 V/μm.[22,24] At these temperatures and field strengths, the cathodes in fluorescent lamps typically supply a lamp current of 0.2–0.4 A.[22–27] For example, Soules *et al.* modeled oxide cathode operation in fluorescent lamps in various operating conditions and found that, in general, the cathode temperature rises to keep up with the increase of lamp current; they also reported cathode temperatures measured with a similar optical pyrometer on cathodes operating at 0.43 A of current, the temperatures of the hottest part of the cathodes are between 1450 and 1600 K in their measurements.[23] Warmouth *et al.* also measured the temperature of a fluorescent cathode operating at 0.27 A as 1 353 K.[26] Similarly, Yamagata *et al.* measured the peak temperature of a cathode operating at around 0.25 A, and their result was 1 390 K.[24] Warmouth also estimated that at around 0.3 A current, the electric field in front of a typical cathode operating in a low-pressure gas discharge environment is around 2.9 V/μm, and the emission current density of the cathode is typically at around 1 A/cm^2.[22,23] The barium strontium oxide-coated CNT cathode, on the other hand, generates an emission current of 0.87 A at similar operating temperature and electric field, which is about three times of the currents from the conventional cathodes reported by these researchers.[22–26] In addition to the examples discussed above, it is also worth noting that compact fluorescent lamps, which use the same type of small triple coiled tungsten filaments used in this study, typically have even lower operating current between 100 and 200 mA of current.[28]

The coiled filament has a complex shape and internal structure than a flat surface so the area of its emission surface is less well defined. By approximating the shape of the filament as a cylinder, we made a generous estimate of the surface area of the filament at around 0.3 cm^2. Assuming this as the area for electron emission, 0.87 A of emission current translates to an estimated current density of 2.9 A/cm^2. However, as only half of the filament facing the anode is likely to emit electrons effectively. So, we have likely overestimated the emission area while underestimated the current density. The actual current density from the cathode is likely higher than this estimated 2.9 A/cm^2 value. Nevertheless, this estimated result is still in line with the current density obtained from a similar barium strontium oxide-coated CNT coating on a flat surface, which is at 4.5 A/cm^2.[17,18] At 2.9 A/cm^2, the emission current density from this cathode is also about three times that of the typical value of 1 A/cm^2 for conventional oxide cathodes.[22]

CNTs themselves are weak thermionic emitters despite the field effect they induce.[6–10] The thermionic emission from CNTs at the comparable temperatures of this study is basically negligible.[6,9,10] This is mainly due to the high work function value of CNTs, which is at around 4.5 eV.[7–10] However, CNTs' surface was altered with a low work function oxide functional coating in this study. The work function of the barium strontium oxide-coated CNT cathode surface was extracted from the I-V plots in Fig. 4(a) using the Richardson line method.[11,12] Figure 4(b) is the Richardson plot for the barium strontium oxide-coated CNT cathode. The equation for the Richardson plot, as shown below, can be easily obtained from Eq. (2),

$$\ln\left(\frac{J_0}{T^2}\right) = -11\,605\,\frac{\varphi}{T} + \ln A_{\text{eff}}. \tag{3}$$

The linear plot of $\ln J_0/T^2$ vs $1/T$, the Richardson plot, has a slope that is equal to $-11\,605\,\varphi$; from the value of the slope of the Richardson plot in Fig. 4(b), the work function of the oxide-coated CNT cathode surface was determined to be 1.6 eV. This is a much-lowered work function value than the work function of the uncoated CNTs, originally at about 4.5 eV. This work function value is comparable to the work functions of typical oxide powder emissive mixtures which are around 1.3–2.5 eV.[19,20,29]

It is quite clear that barium strontium oxide surface coating greatly reduces the work function of the CNTs' surface from about 4.5 to only 1.6 eV as illustrated in this study. It is this modified low work function surface that transforms the thermionic emission properties of the CNTs. The combination of the low work function from the barium strontium oxide coating and the large field effect from the CNTs makes barium strontium oxide-coated CNTs a very strong thermionic emission coating. It not only produces thermionic emission orders of magnitude stronger than that from CNTs[6,9,10] but also leads to an enhanced thermionic emission much stronger than a conventional barium strontium calcium oxide powder mixture.[22–28] The benefits of low work function barium strontium oxide surface coating and a large field effect from the CNTs are both clear. Beyond the immediate application in the thermionic cathode, the implementation of the oxide-coated CNTs in a complex coiled structure is also significant as it demonstrates the adaptability of barium strontium oxide-coated CNTs as a work function lowering and field enhancing functional coating, which may very well be suited for applications in other devices as well.

C. Thermionic cooling effect from barium strontium oxide-coated CNTs

Thermionic cooling is another potential application for barium strontium oxide-coated CNTs. Thermionic cooling occurs when energetic hot electrons emit from the surface and carry energy away. The key to achieve a large thermionic cooling effect is to have a thermionic emission surface that emits hot electrons efficiently. It has been shown previously that a barium strontium

oxide-coated CNTs coating on a flat surface produces a large thermionic cooling effect.[37,38] In this study, even with a complex coiled structure, a large cooling effect is also observed on the barium strontium oxide-coated CNT cathode surface when it emits hot electrons. The top trace in Fig. 5(a) shows the temperature of a cathode (measured at the center point) at various cathode heating current. The temperature of the cathode was raised by this cathode heating current flown through it. As described in Sec. II, this is the temperature of the cathode when there is no voltage bias across the cathode and anode or the temperature of the cathode when thermionic emission is off. The bottom trace in Fig. 5(a) shows the temperature of the cathode when 2 500 V of electric potential bias was applied across the cathode and anode or the temperature of the cathode when thermionic emission is on. Each data point on the curves presents the average temperature of five measurements, and the error bars are the standard deviations of the five temperature readings of each data point on the curves. The cooling of the cathode is apparent, and the effect is strongest when the temperature of the cathode is at its highest. As a hotter surface corresponds to a stronger thermionic emission, so in other words, the largest cooling effect occurs when the thermionic emission is the strongest. The cooling of the cathode is plotted against the thermionic emission current from the cathode in Fig. 5(b). Here, the y axis is the change of the temperature of the cathode and the x axis is the thermionic emission current at which cooling occurs. At 0.91 A of emission current, the temperature of the cathode cooled by 90°.

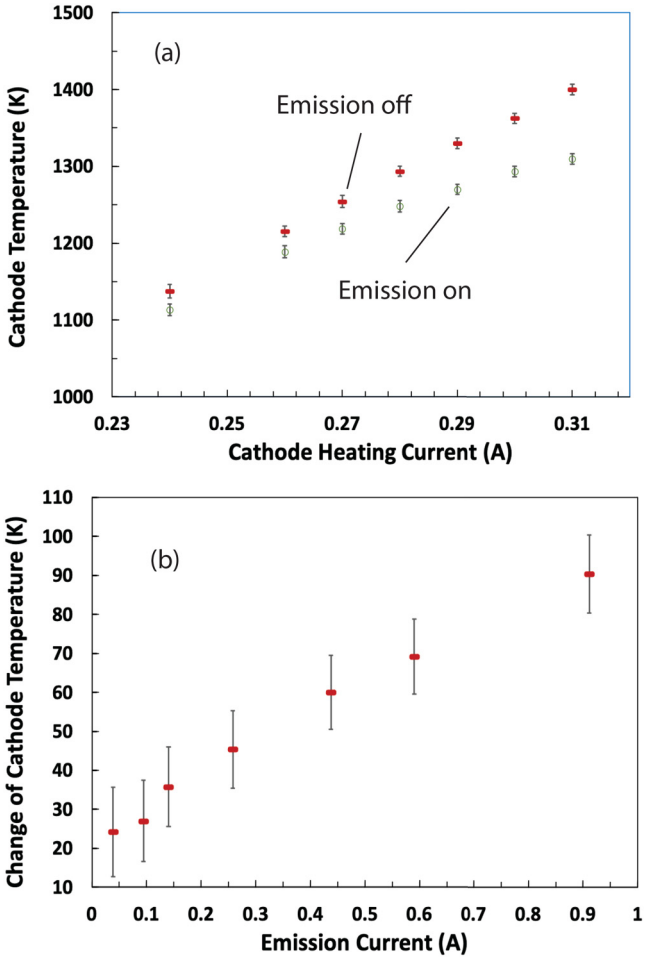

FIG. 5. (a) Temperature of the center point of the barium strontium oxide-coated CNT cathode at various cathode heating current. The top trace is the temperature of the cathode when thermionic emission is off. The bottom trace is the temperature of the cathode when the thermionic emission is on. Each temperature data point represents the average of five measurements and the error bar is the standard deviation of the five measurements. (b) Change of temperature due to thermionic emission from the cathode surface. The y axis is the difference of the two temperature traces above, and the x axis is the corresponding emission current from the cathode at which cooling occurs.

The amount of cooling on the cathode obtained in this study is consistent with the cooling effect of barium strontium oxide-coated CNTs on a flat surface reported earlier.[37] Compared to other experimental results on thermionic cooling in the literature, this is a relatively large cooling effect, even though there is still long way to go before, it can be implemented in practical cooling applications.[30–42] The trend displayed in Fig. 5(b) is clear; the stronger the emission, the larger the cooling effect. The relationship is almost linear in the region of testing in this study. Although the amount of cooling obtained is substantial, this occurs at high temperatures. However, most cooling needs are at more modest temperatures. One possible way to boost the electron emission at lower temperatures further is by increasing the field strength, and this can potentially be accomplished with structures with a narrower gap between the cathode and anode.[43–45] However, as field strength increases, thermionic emission becomes less dominant and eventually transitions to thermal-field and other electron emission mechanisms.[46–48] There have been theoretical analyses attempting to predict whether thermal-field electron emissions of mixed hot and cold electrons will produce a cooling effect on the surface.[49–57] Some analyses indicate cooling by electron emission can be achieved even at room temperature,[52] while others doubt the feasibility of cooling by electron emission at room temperature.[57] Gas breakdown in micro- and nanoscale structures also places a limit on how large a field can be safely applied to a device of a given geometry and operating environment.[47] Another issue with the decreasing gap distance is that as emission increases with a narrower gap and larger field, it may lead to increased space-charge effects.[21,47,48,58] More experimental work seem to be needed to answer some of these questions.

IV. SUMMARY AND CONCLUSIONS

In summary, we have succeeded in implementing barium strontium oxide-coated CNTs as a functional coating onto a coiled tungsten filament to create a new type of thermionic cathode, the barium strontium oxide-coated CNT cathode. The cathode shows strong thermionic emission. At a similar temperature and field strength, this cathode produces a thermionic emission current almost three times that of a typical conventional oxide cathode. This oxide-coated CNT cathode resembles conventional oxide cathodes in the structure, which makes it easier to be adopted in applications.

The strong thermionic emission of this cathode is the result of the combination of the low work function of the barium strontium oxide coating and the high field effect induced by the CNTs. Barium strontium oxide-coated CNTs were grown and fabricated using PECVD and magnetron sputtering deposition, two highly versatile material processing methods. The fact that barium strontium oxide-coated CNTs were able to be incorporated into a rather complex coiled filament structure illustrates the adaptability of this material as a functional coating. It is a relatively portable material that can be deployed in other device applications where a work function lowering and field enhancing functional coating is needed. Thermionic cooling is one of these potential applications. Indeed, a relatively large thermionic cooling was observed on the cathode surface. The temperature of the cathode surface drops as much as 90° when the cathode is emitting a thermionic emission current of 0.91 A.

ACKNOWLEDGMENTS

This material is based upon work supported, in part, by the U.S. Department of Energy under Award No. DE-FC26-04NT 42329.

DATA AVAILABILITY

The data that support the findings of this study are available from the corresponding author upon reasonable request.

REFERENCES

[1]S. H. Jo, D. Z. Wang, J. Y. Huang, W. Z. Li, K. Kempa, and Z. F. Ren, Appl. Phys. Lett. **85**, 810 (2004).
[2]S. H. Jo, Y. Tu, Z. P. Huang, D. L. Carnahan, D. Z. Wang, and Z. F. Ren, Appl. Phys. Lett. **84**, 413 (2004).
[3]S. H. Jo, Y. Tu, Z. P. Huang, D. L. Carnahan, D. Z. Wang, and Z. F. Ren, Appl. Phys. Lett. **82**, 3520 (2003).
[4]Yan Chen, David T. Shaw, and Liping Guo, Appl. Phys. Lett. **76**, 2469 (2000).
[5]K. B. K. Teo, M. Chhowalla, G. A. Amaratunga, W. I. Miline, G. Pirio, P. Legagneux, F. Wyczisk, D. Pribat, and D. G. Hasko, Appl. Phys. Lett. **80**, 2011 (2002).
[6]D. C. Cox, R. D. Forrest, P. R. Smith, and S. R. R. Silva, Appl. Phys. Lett. **85**, 2065 (2004).
[7]M. Shiraishi and M. Ata, Carbon **39**, 1913 (2001).
[8]L. Xiao, P. Liu, L. Liu, K. Jiang, X. Feng, Y. Wei, L. Qian, S. Fan, and T. Zhang, Appl. Phys. Lett. **92**, 133108 (2008).
[9]F. Jin, Y. Liu, and C. Day, Appl. Phys. Lett. **88**, 163116 (2006).
[10]F. Jin, Y. Liu, C. Day, and S. Little, Carbon **45**, 587 (2007).
[11]I. G. Herrmann and P. S. Wagener, *The Oxide-Coated Cathode* (Chapman & Hall, London, 1951), Vol. 2, pp. 77–75, 178–181.
[12]R. O. Jenjins, Vacuum **19**, 353 (1969).
[13]M. Mostafa and S. Banerjee, J. Appl. Phys. **115**, 244309 (2014).
[14]J. D. Correa and W. Orellana, J. Appl. Phys. **113**, 174305 (2013).
[15]V. Georgakilas, K. Kordatos, M. Prato, D. M. Guldi, M. Holzinger, and A. Hirsch, J. Am. Chem. Soc. **124**, 760 (2002).
[16]V. V. Dobrokhotov and C. A. Berven, Phys. E **31**, 160 (2006).
[17]F. Jin and A. Beaver, J. Vac. Sci. Technol. B **35**, 041202 (2017).
[18]F. Jin and A. Beaver, Appl. Phys. Lett. **110**, 213109 (2017).
[19]J. Gao, Y. Yang, X. Zhang, S. Li, P. Hu, and J. Wang, Tungsten **2**, 289 (2020).
[20]G. Gaertner and D. D. Engelsen, Appl. Surf. Sci. **251**, 24 (2005).
[21]P. Zhang, Y. S. Ang, A. L. Garner, Á Valfells, J. W. Luginsland, and L. K. Ang, J. Appl. Phys. **129**, 100902 (2021).
[22]J. F. Waymouth, *Electric Discharge Lamps* (MIT, Cambridge, MA, 1971), pp. 71–113.
[23]T. F. Soules, J. H. Ingold, A. K. Bhattacharya, and R. R. Springer, J. Illum. Eng. Soc. **18**, 81 (1989).
[24]Y. Yamagata, M. Kai, S. Naito, K. Tomita, K. Uchino, and Y. Manabe, Thin Solid Films **18**, 3449 (2010).
[25]R. Garner, J. Phys. D: Appl. Phys. **41**, 144009 (2008).
[26]R. Nachtrieb, F. Khan, and J. Wamouth, J. Phys. D: Appl. Phys. **38**, 3226 (2005).
[27]S. Hadrath, R. C. Garner, G. H. Liedar, and J. Ehlbeck, J. Phys. D: Appl. Phys. **40**, 6975 (2007).
[28]J. Cunill-Sola and M. Saliches, IEEE Trans. Power Delivery **22**, 2305 (2007).
[29]K. C. Mishra, R. Garner, and P. C. Schmidt, J. Appl. Phys. **95**, 3069 (2004).
[30]V. Garimella, Y. K. Joshi, A. Bar-Cohen, K. C. Toh, V. P. Parey, M. Baelmans, J. Lohan, B. Sammakia, and F. Andros, IEEE Trans. Compon. Packag. Technol. **25**, 569 (2002).
[31]G. Chen and A. Shakouri, Trans. ASME **124**, 242 (2002).
[32]G. D. Mahan, J. Appl. Phys. **76**, 4362 (1994).
[33]G. D. Mahan and L. M. Woods, Phys. Rev. Lett. **80**, 4016 (1998).
[34]G. D. Mahan, J. O. Sofo, and M. Bartkowiak, J. Appl. Phys. **83**, 4683 (1998).
[35]A. Shakouri and J. E. Bowers, Appl. Phys. Lett. **71**, 1234 (1997).
[36]A. Shakouri, C. LaBounty, J. Piprek, P. Abraham, and J. E. Bowers, Appl. Phys. Lett. **74**, 88 (1999).
[37]F. Jin and S. Little, Appl. Phys. Lett. **106**, 113102 (2015).
[38]F. Jin and D. Carter, J. Vac. Sci. Technol. B **36**, 051804 (2018).
[39]T. P. Lin and G. Eng, J. Appl. Phys. **65**, 3205 (1989).
[40]Y. Hishinuma, T. H. Geballe, and B. Moyzhes, J. Appl. Phys. **94**, 4690 (2003).
[41]L. W. Swanson, L. C. Crouser, and F. M. Charbonnier, Phys. Rev. **151**, 327 (1966).
[42]F. M. Charbonnier, R. W. Strayer, L. W. Swanson, and E. E. Martin, Phys. Rev. Lett. **13**, 397 (1964).
[43]Y. Hishinuma, T. H. Geballe, B. Moyzhes, and T. W. Kenny, Appl. Phys. Lett. **78**, 2572 (2001).
[44]Y. Hishinuma, B. Moyzhes, and T. H. Geballe, Appl. Phys. Lett. **81**, 4242 (2002).
[45]A. N. Korotkov and K. K. Likharev, Appl. Phys. Lett. **5**, 2491 (1999).
[46]K. L. Jensen, IEEE Trans. Plasma Sci. **46**, 1881 (2018).
[47]A. L. Garner, G. Meng, Y. Fu, A. M. Loveless, R. S. Brayfield II, and A. M. Darr, J. Appl. Phys. **128**, 210903 (2020).
[48]A. M. Darr, C. R. Darr, and A. L. Garner, Phys. Rev. Res. **2**, 033137 (2020).
[49]A. N. Korotkov and K. K. Likharev, Appl. Phys. Lett. **75**, 2491 (1999).
[50]P. Lyu and C. Zhang, Appl. Phys. Lett. **89**, 153125 (2006).
[51]L. Wu and L. K. Ang, Appl. Phys. Lett. **89**, 133503 (2006).
[52]T. D. Musho, W. F. Paxton, J. L. Davidson, and D. G. Walker, J. Vac. Sci. Technol. B **31**, 021401 (2013).
[53]T. S. Fishers and D. G. Walker, Trans. ASME **124**, 954 (2002).
[54]T. S. Fishers, Appl. Phys. Lett. **79**, 3699 (2001).
[55]M. S. Chung, S. C. Hong, A. Mayer, P. H. Cutler, B. L. Weiss, and N. M. Miskovsky, Appl. Phys. Lett. **92**, 083505 (2008).
[56]H. T. Chua, X. Wang, and J. M. Gordon, Appl. Phys. Lett. **84**, 3999 (2004).
[57]M. S. Chung, J. Y. Choi, A. Mayer, N. M. Miskovsky, and P. H. Cutler, Appl. Phys. Lett. **104**, 083502 (2014).
[58]Y. Y. Lau and Y. Liu, Phys. Plasmas **1**, 2082 (1994).